

Investigation into Morphology of Cavitation Erosion-Corrosion Pits on the Surface of Carbon Steel

Salem. A. Karrab
Misurata University /
Department of Materials
Science and Engineering
Misurata - Libya
sgarrab2005@yahoo.co.uk

Mohammed S. Aboraia
Assiut University /
Department of Mining &
Material Engineering
Assiut - Egypt
maboraia@hotmail.com

Mohammed. A. Doheim
Assiut University /
Department of Mining &
Material Engineering
Assiut - Egypt
mohdoheim@yahoo.com

Shemy M. Ahmed
Majmaah University /
Department of Mechanical
Engineering
Majmaah - KSA
shemy2007@yahoo.com

Abstract — Nano-sized films associated with the ring areas formed around micropits in cavitation erosion experiments were investigated. The corrosion behavior and vibratory cavitation erosion tests of mild carbon steel in 3% NaCl distilled water were carried out. The results showed that the nano-sized films associated with the ring areas formed around micropits in cavitation and free cavitation tests have a similar shape. The study proved that the nano-structure and the ring areas formed around micropits are the result of corrosion effects and not as a result of thermal effects related to the collapse of the bubbles.

Index Terms — Cavitation erosion, pit, carbon steel.

I. INTRODUCTION

Vibratory cavitation erosion tests are the most commonly laboratory devices used for studying the cavitation erosion aspects, Since it is easy to obtain some erosion data within a relatively short test time [1]. In this test method, the horn-tip is immersed in the liquid and is vibrated at high frequency, which makes damage to the surface of the horn-tip damages or other surface closed to the horn-tip. The vibration generates rarefaction and compression waves in the liquid. These waves induce the formation and collapse of cavities in the liquid, and the collapsing cavities produce the damage and erosion of the specimen. Such test has disadvantage that the data do not consider the cavitation number σ as a controlling factor of the erosion mechanism. Therefore, it cannot accurately simulate the actual rate of the mechanism that was occurring in the cavitating field, although the nature of the material damage mechanism seems almost similar [2].

According to the literature, the cavitation damage process of ductile materials is divided into the following periods: (I) incubation period; (II) acceleration period; (III) steady-state period (IV) attenuation period. In incubation period, the damage features include extensive plastic deformation of surface regions combined with

little particle removal, the formation of pits, surface depressions and crack initiation at regions of high stress concentration. In the acceleration period (II), the erosion rate increases to its maximum level because of superficial hardening and crack development. In the steady-state period (III), the erosion rate is the greatest and has a constant value which can be related to the attack on homogenous work-hardened surface. In attenuation period (IV), the erosion rate decreases associated with a reduction in the damage and a reduction of cavitation collapse pressure. This is attenuated by the existence of cavities in the vicinity of rough surface, and cushioning effect of liquid trapped in the pockets and crevices of the eroded surface or the cushioning effect of diffused air in liquid at the cavitation zone.

Pits formed individually during the incubation period are an important mean to evaluate cavitation fields and material [3-6]. However, many aspects of pits are still vague or debatable and controversial since their generation process is complex. The pit features include; size, depth, shape, mechanism of formation, role of pits in developing erosion and their clustering. Another problem escalated recently about the type of pit, which was formed during cavitation, whether it belongs to the cavitation or corrosion.

The aim of the present work is to through more light on the morphology of cavitation erosion pit, corrosion pit and their interaction formed on carbon steel cavitated in 3% NaCl. From morphology of pit formation, the ring area formed around cavity and nano sandwich sheets generated within ring area will be clarified.

A. Pit Characteristics

The pit's size (d_o) formed by vibratory cavitation erosion is in the range of few micrometers [7-13]. This size's range of pit seems to be acceptable and can be interpreted as follow: the bubbles in form of clusters [14] have an initial diameter, d_o of the millimeter range. Microjet formed by those bubbles will have diameters d_j of the order of $d_o/50$ according to Plesset and Mitchell's theory [15]. Microjet diameters might further decrease within the boundary layer on the specimen surface by a factor of 10. Thus, the diameter d_j is roughly evaluated to be several micrometers. Therefore, the microjet could be

Received 1 September 2014; revised 20 September 2014; accepted 17 October 2014.

Available online 19 October 2014.

responsible for such tiny pit. On the other hand, it is reported in the literature that the pit may be two figures, i.e. in the range of 25 μm [13,16]. This kind of pits is formed as result of shock wave and has common features of plastic deformation and shallow appearance [13]. For the pit's shape, it is recognized that is irregular [7-13]. To the author's knowledge, there is no plausible explanation to the irregularity of pits reported in the literature; however it is believed that the irregularity is associated with the bubble collapse process and material surface properties.

The role of pits on erosion or development of erosion lies in the definition of the size scale of the pit. So it must be differentiated between the pit caused by the microjet and the other resulting from the plastic deformation, and large-size. The larger-size pit, under scanning electron microscope, formed through the stages of development of surface hardening to plastic lines, the crack nucleation, the crack propagation and the fall of the particles [13,17]. That is the predominant failure mode in cavitation erosion is fatigue failure. The pit morphology, the pit number and its rule in developing erosion has studied by one of authors [12,13]. The systematic observation of the feature of micro-jet pits with the testing time showed that the sizes and shapes of microjet pits did not change at all and the rate of formation of pits with test time was initially high then decreased. Such pits scarcely played an important role in developing erosion [12,13,18]. To characterize the predominant cavitation erosion mechanism, Ahmed et al. [13,14, 17, 19-23] carried out systematic observations on eroded surfaces and dislodged particles for different materials cavitated in different liquids. They clearly showed that the predominant failure mode in cavitation erosion was fatigue. There are also many research experimentally and numerically found that fatigue is a mechanism of cavitation erosion [24-27].

Recently, some researchers have noted that rings with iridescent color around the pits formed in their experiments by a rotating-disk [28] or vibratory test rig [29-34]. They assumed that the cause of the rings that have formed around the erosion pits due to the thermal effects related to the collapse of bubbles above those rings. Li et al [33] reported that concentric iridescent rings around the erosion pit make it different from those corrosion pits. They added that the difference by the distinct color and the $\alpha\text{-FeOOH}$ structure of the rings indicated that the iridescent rings (figure 1 taken from Ref. [33]) were oxidation film formed under high temperature generated in the cavitation environment. Another observation reported by Yan et al. [34] that nano sandwich sheets generated in ring area around cavitation erosion pit on the surface of carbon steel. On the other hand, Karrab et al. [35] investigated the ring areas formed around micropits in cavitation erosion experiments by carrying out corrosion behavior and vibratory cavitation erosion tests of mild carbon steel in tap and distilled water. Their results showed that the ring areas were densely formed in tap water and scarcely formed in distilled water in cavitation tests. The ring areas formed around micropits in cavitation and free cavitation tests

have a similar shape. Moreover, scanning electron microscopic (SEM) examinations showed that the corrosion products spread within the ring areas. Thus, the ring areas formed around micropits are the result of corrosion effect and are not the result of thermal effects due to bubble collapse.

Pitting corrosion morphology has been considered extensively in literature for different materials and under different conditions. The film formed around the pit is due to corrosion products as reported in numerous researches on pure corrosion [36-41]. Here, pitting corrosion on a stainless steel bar exposed to an alkaline solution loaded with chlorides is depicted in Fig. 2. [42]. Despite the difference in materials and test conditions for the pits shown in Figs 1 and 2, but it is clear that there are an identical between the pitting corrosion and corrosion pits formed under cavitation test. That means, that the circular area that formed around the cavity at the center formed as a result of corrosion and have no relationship with cavitation. For the microstructure of the film formed around micropit has also been studied for carbon steel corroded in atmosphere by Kui et al. [43]. They concluded that the ring-shaped products were composed of lepidocrocite ($\gamma\text{-FeOOH}$) and magnetite ($\gamma\text{-Fe}_2\text{O}_3$) transformed from lepidocrocite.

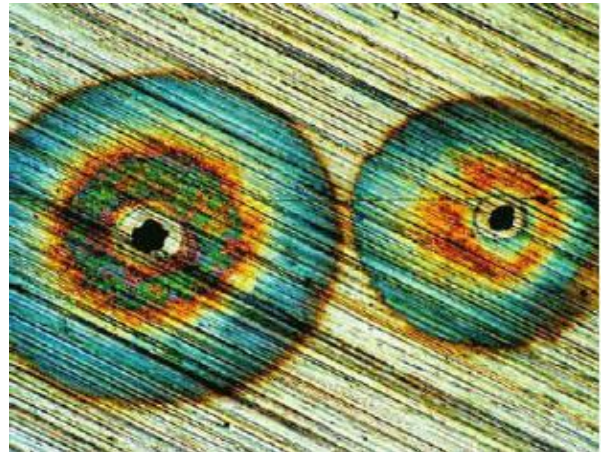


Figure 1. Illustrating the corrosion pit formed during cavitation test [33]

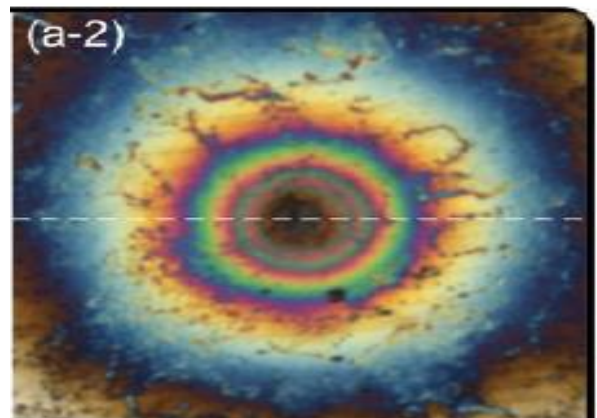


Figure 2. Pitting corrosion [42]

After an electroless Ni-P plating on carbon steel in the author's lab [44], the immersion test in tap water were carried out to identify the defects of plating. By

examining the surface of plating, it was observed that many corrosion pits were formed. The image shown in Figure 3 indicates clearly the iridescent rings that were formed around center's cavity and basically axial symmetric. The image illustrates that the number of iridescent rings are different among pits. This means that the number of iridescent rings is not inherent to cavitation bubble collapse. The number of iridescent rings depends on the potential distribution which is not uniform and the thickness of the oxide that will increase with increasing distance from the pit center [45]. This invalidates the assumption that the formation of the iridescent rings was attributed to the repeated interactions between mechanical removal and high temperature oxidation during the cavitation erosion reported by Li et al. [33]

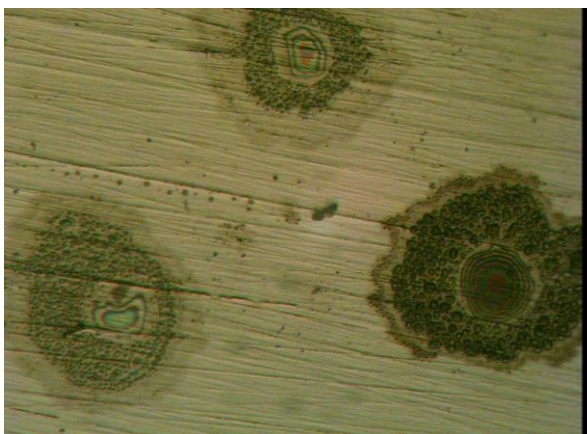


Figure 3. Pitting corrosion morphology observed on electroless Ni-P plating after dipping in tap water

It is worth noting that these researchers [29-34] who claim that the ring area is a result of the collapse of bubbles, the intensity of vibration cavitation was low in all their experiments. The amplitude of vibrations was in the range of 6-12 micrometers. While the ASTM standard test conditions [2] apply the peak-to-peak displacement amplitude of the test surface of the specimen shall be 50 μm . Moreover, in some experiments where they used stationary-specimen method, the standoff distance is too large reached 40 mm, leading undoubtedly to reduce intensity of cavitation [46]. Thus, the prevailing mechanism to ring-area formation in these researches is the corrosion.

II. EXPERIMENTAL

Cavitation experiments were carried out using a vibratory cavitation apparatus employing the stationary specimen. A schematic diagram of the test equipment is shown in Figure 4. The device consists of a piezoelectric transducer oscillating at $20 \text{ kHz} \pm 50 \text{ Hz}$ frequency and a horn which amplifies the vibration amplitude. The horn tip was made of a cavitation resistant material and it had a flat head as well as its dimensions are shown in Figure

4(b). The specimen was placed coaxially with the horn and was held stationary at the distance L from the horn tip as shown in Figure 4 (a). The flat face of the vibrating tip generates suction during its upward motion under liquid, which results in the creation of vapor-filled bubbles collectively known as a cavitation zone. That zone collapses during the subsequent downward motion. Cavitation damage occurs on the vibrating tip and on the stationary specimen. However, the damage that occurs on the horn tip is negligible compared with that occurs on the stationary one. Thus peak-to-peak amplitude of vibration of the horn tip was 50 μm . The separation distances L between the specimen and the end of vibrating tip was initially adjusted using dial gage and maintained at the value of 0.8 mm, in the present study, to obtain significant values of erosion damage [46]. This experimental procedure is conforming to ASTM standard G32-09 [2].

A3 wt % solution of NaCl in distilled water was used as cavitating liquids. The salt water solution was made with reagent grade NaCl. The specimen and the end of the horn tip were immersed in 1200 ml open beaker, containing 700 ml of the test liquid. Since the temperature change will affect the physical properties of the test liquid such as dissolved gas, pH, surface tension and vapor pressure, the degree of erosion [47] and corrosion [48] as well as their interaction will be undoubtedly changed. Therefore, the test liquid temperature was kept constant at $27 \pm 1 \text{ }^\circ\text{C}$, by circulating cooling water around the beaker, as shown in Figure 4(a). Preliminary tests showed that temperature of the liquid film on the specimen surface rose rapidly. Regardless of the constant temperature in the beaker, this temperature is measured for a maximum duration test time with a thermocouple inserted in the center of test piece. It was found for 10 min. (maximum interval test time), that the film temperature did not exceed the controlled temperature of beaker by more than $2 \text{ }^\circ\text{C}$.

The specimens were made of AISI-1045 carbon steel whose corrosion damage is easily detectable because of its low-corrosion resistance. The chemical composition and the mechanical properties are listed in Tables [1] and [2] [49]. The metallographic structure of AISI 1045 carbon steel is given in Figure 5. The microstructure composes of (white) pearlite and (dark) ferrite. The specimens were flat-surfaced discs of 14 mm in diameter and 10mm height and were cut from a single rod (as cast) to ensure metallurgical uniformity. Since the surface roughness plays an important role in developing the erosion and material removal [19], therefore, the specimen's working faces were polished with grade 3000 dry emery paper to ensure average roughness R_a within $0.08 \text{ } \mu\text{m}$. Before and after each test, the specimens were rinsed in acetone and dried in air and weighed with a $100 \text{ g} \pm 0.1 \text{ mg}$ sensitivity balance. The corrosion experiment in static salt water was also performed on the specimens (with the same set as in cavitation test but without vibration) to give a complete picture on the pit formation. The damaged surfaces were examined using SEM (JEOL JSM 5400) and optical microscope (OM).

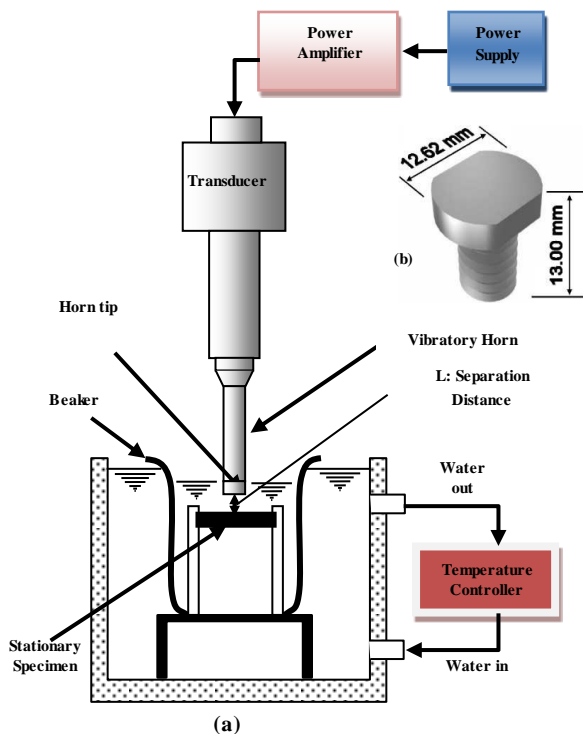


Figure 4 Schematic diagram for an ultrasonic vibratory facility (a) Schematic view of test apparatus, (b) Horn's disc

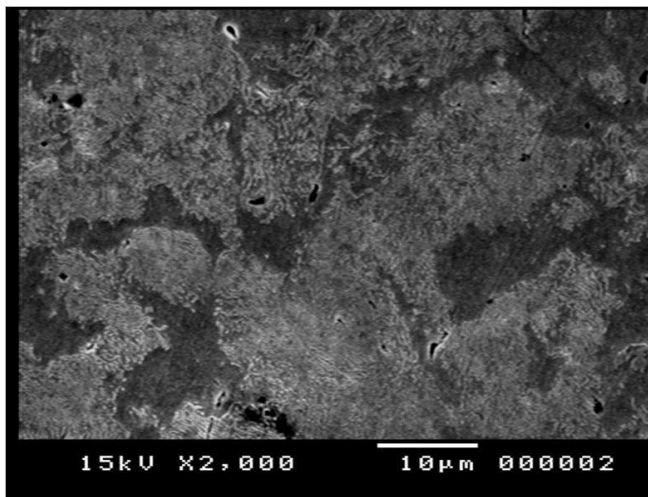


Figure 5 SEM photograph showing the microstructure of steel AISI-1045 with (white) pearlite and (dark) ferrite

III. Results and Discussion

A. Pitting Corrosion

The typical corrosion pits formed on the specimens of carbon steel after 20 min. immersed in salt water, as observed by SEM, are shown in Figure 6. As evident from Figure 6 that the pits appear as dispersed white areas and have different sizes ranged from few micrometers to the order of one hundred micrometers. The small sizes are individual pits, while, the larger sizes represent the interaction amongst the localized corrosion sites. Closer

observation to individual pits illustrates that the characteristic features of these pits are the presence of two parts: a cavity at the pit centre of darker appearance and a white ring zone around the cavity. The size of cavity is in order of 1 μm . The cavity is a chemical or physical heterogeneity at the surface such as inclusions, second-phase particles, solute-segregated grain boundary, flaws and mechanical damage or dislocations [50]. For both carbon steel and stainless steel, sulfide inclusions, e.g. manganese sulfide MnS [51], are common locations for the initiation of corrosion pits. All steels contain sulfur impurities and due to the low solubility of sulfides, sulfide inclusions are formed. In carbon steels, the attack initiates in the matrix close to the sulfide inclusion, which is more noble than the matrix. For the ring areas, their sizes depend on the test liquid and on the potential differences that exist between different micro-zones on the test surface. The speculator has found that the ring area formed in salt water differed from that in tap water. This difference returns to the propagation of pit and the dissolution of oxide film around the pits due to a high conductivity of salt water. This is in agreement with that reported by Shreir [52] if a tantalum-platinum bi-electrode (1 \times 1 inch tantalum with platinum, 0.1 \times 0.1 inch, welded to the centre) is anodically polarized in sea-water only a first-order blue film will be formed uniformly on the tantalum surface and current will then proceed through the platinum. In a low-conductivity water, however, the potential distribution is not uniform and the thickness of the oxide will increase with increasing distance from the platinum microelectrode. This results in a wedge-shaped oxide film which gives rise to five orders of interference as a series of concentric rings around the platinum.

For the spatial interaction amongst localized corrosion sites will be highlighted from magnified photos shown in Figure 7. This interaction seems in the form of satellite pits, labeled P_s , that tend to form patterns around larger primary pits, labeled P_L . This is in agreement with that reported in the literature [40, 51]. Pitting is considered to be autocatalytic in nature; once a pit starts to grow, the conditions developed are such that further pit growth is promoted as reported by Frankel [53]. This can be explained [52], when a pit begins to form, the local environment changes. Concentration changes in solution occur when metal cations enter solution and hydrolyze, bringing about an increase in both the local chloride concentration and local acidity. The environment in this way becomes more aggressive. Solution concentration and potential gradients develop that can affect pitting susceptibility on adjacent surfaces. These factors can also affect nearby oxide films and non-metallic inclusions to produce more permanent interactions. Taking into account these local changes, pitting can have a significant influence on the susceptibility of adjacent surfaces to localized corrosion. However, the time constant associated with each of these interactive processes differs.

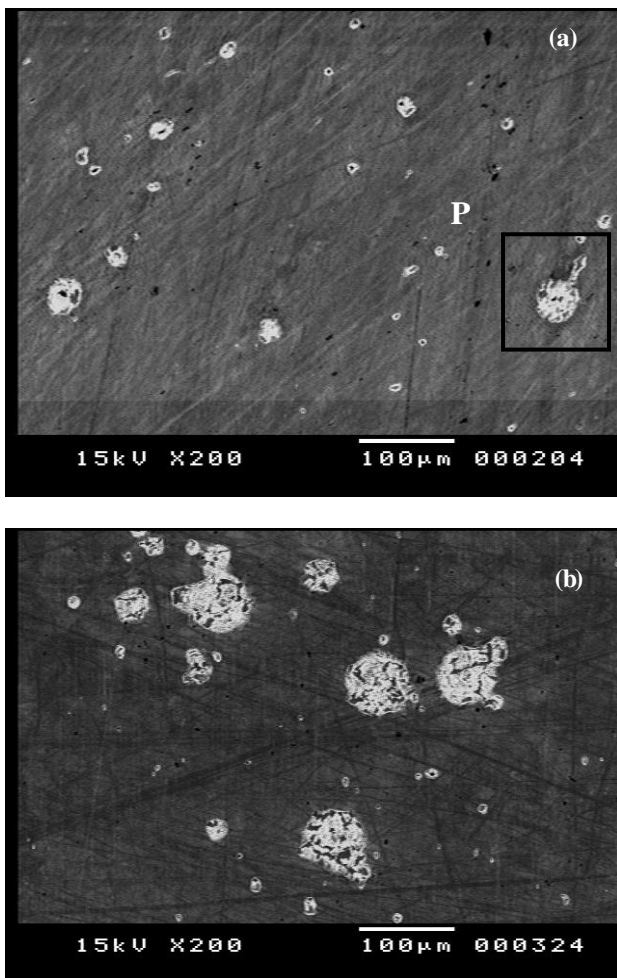


Figure 6. Corrosion pits formed at different positions on the steel surface at stationary conditions in salt water

Figure 7 shows another important feature, is a formation of dense nano-sized films around pit. For more clarity some of pits with nanostructure are magnified as shown in Figures 8 and 9.



Figure 7 High magnification for the pits (P) showing the pitting interactions

These nano-sized films formed as result of corrosion for different materials and for different conditions have extensively observed in literature [54-56]. Therefore, It can be concluded that the nano-sized films formed on the damaged surface are not related to cavitation as reported by Yan et al.[34]. The formation of the nano-sized films on the damaged surface is as result of the dissolution of oxide films around the pits.

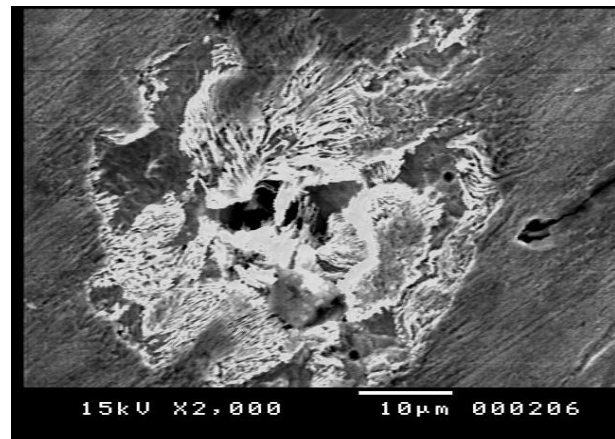


Figure 8. Formation of nano-sized films around pitting corrosion

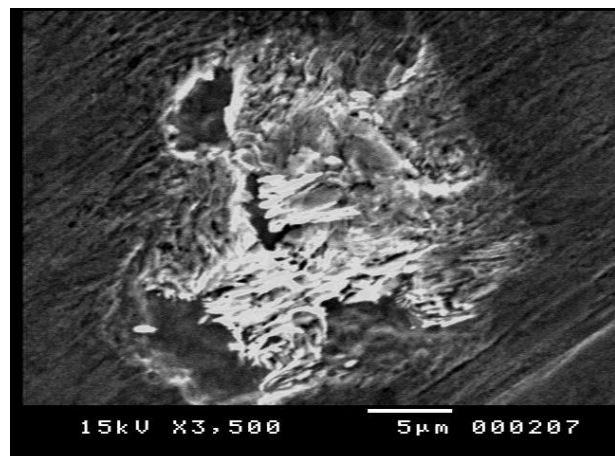


Figure 9. Formation of nano-sized films around pitting corrosion

B. Morphology Of Cavitation Erosion-Corrosion Pit

Figure 10 (a-d) presents the cavitation erosion-corrosion pit formed on carbon steel at test time of 20 min. Figures 10(a) and 10(b) have the same magnification, but, the development of the two pits are different. Figures 10(c) and 10 (d) have also the same magnification, but larger than that in Figures 10(a) and 10(b). All the photos of pits show the nano-sized films formed around the pits. The removal of nano-sized films differed from pit to another. From Figures 10 (a) and 10(c), it can be observed the corrosion products in the center of pits, which confirm the electrochemical effect. By comparing Figure 10 and Figures 7 and 8, with the exclusion of removal that occurred as a result of cavitation in the Figures 10-13, it is easy to find similarities in the formation of pitting.

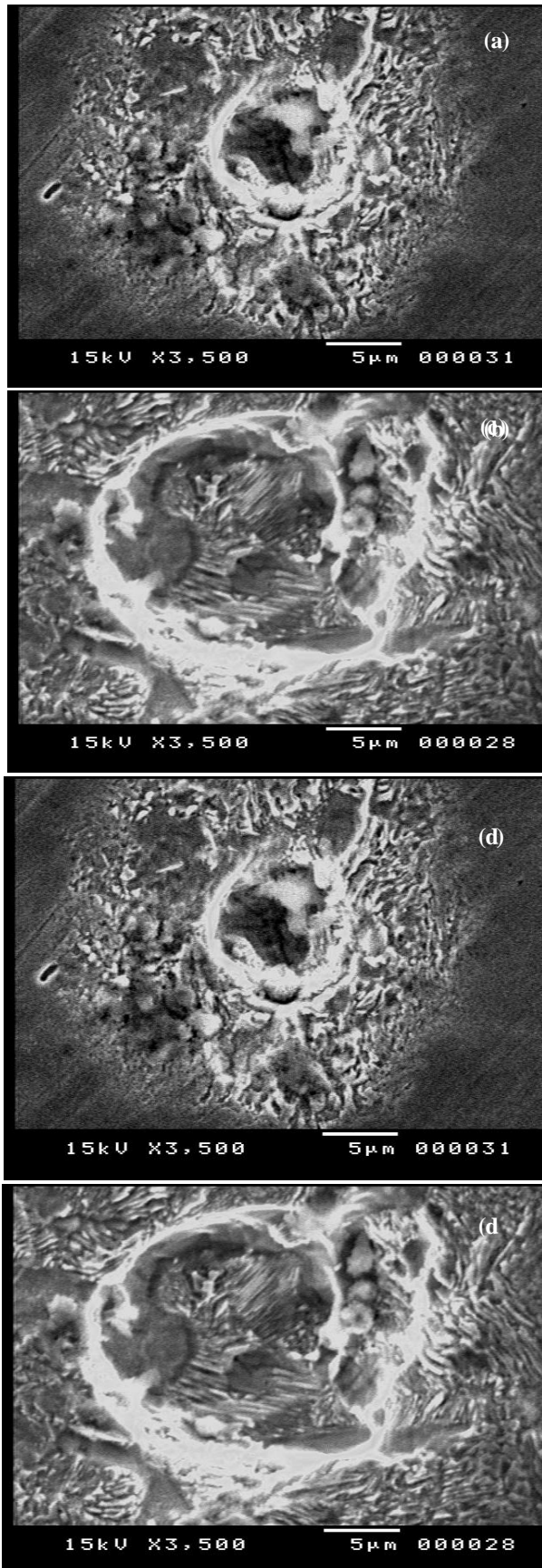


Figure 10 Represent the cavitation erosion-corrosion pit

This means that the ring areas or nano-sized films around pit are formed as result of pure corrosion. These results for salt water accentuate the previous finding [35] that the ring areas were densely formed in tap water and scarcely formed in distilled water in cavitation tests. The ring areas formed around micropits in cavitation and free cavitation tests have a similar shape.

Based upon the above analysis on the ring areas and nano-sized films associated with thosering areas formed around pit or cavity, it can be stated that the ring area is an electrochemical effect and not a thermal effect as reported by Chen et al. [29-34]. However, the role of cavitation shock wave or micro-jet enhances corrosion in removing the nano-sized films formed as result of electrochemical effect.

IV. CONCLUSIONS

1. The nano-sized films or nano structure associated with ring areas are resulted from electrochemical effect and are not related to cavitation. However, cavitation enhances the removal of nano-sized films.
2. The iridescent color of the ring areas are related to the potential distribution of oxide films around the pit, and are not related to the thermal effect of bubble collapses.
3. The ring areas formed around micropit in free cavitation or with cavitation are similar and resulted from electrochemical effect

REFERENCES

- [1] R. T. Knapp, J.W. Daily, F.G. Hammit, "Cavitation," McGraw-Hill, New York. 1970.
- [2] ASTM G 32-09, 2009 "Standard test method for cavitation erosion using vibratory apparatus" Annual book of ASTM standards, Philadelphia, PA.
- [3] R.T. Knapp, "Recent Investigation on the Mechanics of Cavitation and Erosion Damage," Trans. ASME. 77, pp.1045-1054, 1955.
- [4] B. Belahadji, J. P., Franc, J. M., Michel, "Statistical analysis of cavitation erosion pits," ASME J. Fluids Eng. 113, pp.700-706, 1991.
- [5] J. P. Frank, "Incubation time and cavitation erosion rate of work hardening materials," ASME J. Fluids Eng. 113, pp. 021303-1-14, 2009.
- [6] A. Jayaprakash, et al., "Scaling study of cavitation pitting from cavitating jets and ultrasonic horns," Wear 296, pp. 619-629, 2012.
- [7] S., Vaidya, and C.M. Preece, "Cavitation erosion of age-hardenable-aluminum alloys", Metall. Trans. A, 9A, pp. 299-307, 1978.
- [8] E. H. R. Wade, and C. M., Preece, "Cavitation erosion of iron and steel", Metall. Trans. A, 9A, pp.1299-1310, 1978.
- [9] B. Vyas, and C. M. Preece, "Cavitation erosion of face centered cubic metals," Metall. Trans. A, 8A, pp. 915-923, 1977.
- [10] I. Okada, J. Iwamoto, and K., Sano, "Fundamental studies on cavitation erosion-: Observation of the eroded surface by scanning electron microscopy," Bull. JSME, 20(147), pp. 1067-1075, 1977.
- [11] S. Hattori, and E. Nakao, "Cavitation erosion mechanisms and quantitative valuation based on erosion particles," Wear, 249, pp. 839-845, 2001.
- [12] S. M. Ahmed, K. Hokkirigawa, Y. Ito, R. Oba, Y. Matsudaira, "Scanning electron microscopy observation on the incubation period of vibratory cavitation erosion," Wear 142, pp. 303-314, 1991.

- [13] A. Abouel-Kasem, A. Ezz El-Deen, K. M. Emara, S. M. Ahmed, "Investigation into cavitation erosion pits," *ASME J. Tribol.* 131, pp. 031605- 1-031605-7, 2012
- [14] A. Abouel-Kasem, S. M., Ahmed, "Bubble structures between two walls in ultrasonic cavitation erosion into cavitation erosion pits," *ASME J. Tribol.* 134, pp. 021702- 1-021702-9, 2012.
- [15] Plesset, M.S., Michel, T.P., 1956, "On the stability of the spherical shape of vapor cavity in a liquid", *Q. Appl. Math.* 13, pp. 419-430.
- [16] I. Hansson, and K. A. Morch, "Comparison of the initial stage of vibration and flow cavitation erosion," in *Proc. of 5th Intern. Conf. on Erosion by Solid Impact*, Cavendish Laboratory, Cambridge, UK, Paper No. 60. 1979.
- [17] S. M. Ahmed, K. Hokkirigawa, and R. Oba, "Fatigue failure of SUS304 caused by vibratory cavitation erosion," *Wear*, 177, pp. 129-137, 1994.
- [18] A. Karimi, and F. Avellan, "Comparison of erosion mechanisms in different types of cavitation," *Wear*, 113, pp. 305-322, 1986.
- [19] S.M. Ahmed, K. Hokkirigawa, R. Oba, K. Kikuchi, "SEM observation of vibratory cavitation fracture mode during the incubation period and the small roughness effect," *JSME Int. J. Ser. II* 34(3), pp. 298. 1991.
- [20] A. Abouel-Kasem, S. M., Ahmed, "Cavitation erosion mechanism based on analysis of erosion particles," *Trans. ASME, J. Tribol.*, 130, pp. 031601, 2008.
- [21] A. Abouel-Kasem, K. M. Emara, S. M. Ahmed, "Characterizing cavitation erosion particles by analysis of SEM image," *Tribol. Int.*, 42, pp.130-36, 2009.
- [22] A. Abouel-Kasem, S. Baha, S. M. Ahmed, "Quantitative analysis of cavitation erosion particle morphology in dilute emulsions," *Trans. ASME, J. Tribol.*, 130, pp. 041603-1, 2008.
- [23] B. Saleh, A. Abouel-Kasem, A., Ezz El-Deen, S.M., Ahmed, "Investigation of temperature effects on cavitation erosion behavior based on analysis of erosion particles," *Trans. ASME J. Tribol.* 132, pp. 031601, 2010.
- [24] S., Vaidya, C. M., Preece, "Cavitation erosion of age-hardenable aluminum alloys," *Metall. Trans. A*, 9A, 299-307, 1978..
- [25] H.R. Wade, C.M. Preece, "Cavitation erosion of iron and steel," *Metal Trans*, 9A, pp.1299-1310, 1978.
- [26] W. Bedkowski, et al., "Relations between cavitation erosion resistance of materials and their fatigue strength under random loading," *Wear*, 230, pp. 201-209, 1999.
- [27] W. Bedkowski, et al., "Relations between cavitation erosion resistance of materials and their fatigue strength under random loading," *Wear*, 230, pp. 201-209, 1999.
- [28] H., Chen, "Iridescent rings around cavitation erosion pits on surface of mild carbon steel," *Wear* 269, pp. 602–606, 2010.
- [29] H. Chen, J. Li, D., Chen, J. Wang, "Damages on steel surface at the incubation stage of the vibration cavitation erosion in water," *Wear* 265, pp. 692–698, 2008.
- [30] H. Chen, J. Li, D., Chen, J. Wang, "Affected zone generated around the erosion pit on carbon steel surface at the incipient stage of vibration cavitation", *Chin. Sci. Bull.* 53, pp. 943–947, 2008.
- [31] H. Chen, J. Li, "A ring area formed around the erosion pit on 1Cr18Ni9Ti stainless steel surface in incipient cavitation erosion," *Wear* 266, pp. 884-887, 2008.
- [32] H. Chen, J. Li, S. H. Liu, "Thermal effect at the incipient stage of cavitation erosion on a stainless steel," *J. Fluid Eng.* 231, pp. 1-3 2009.
- [33] J. Li, B. Wu, H. Chen, "Formation and development of iridescent rings around cavitation erosion pits," *Tribol. Lett.* 52, pp. 495-500. 2013.
- [34] D. Yan, J. Wang, F. Liu, D. Chen, "The generation of nano sandwich sheets in ring area around cavitation erosion pit on the surface of carbon steel," *Wear* 303, pp. 419–425., 2013.
- [35] S.A. Karrab, M.A. Doheim, S. Mohamed, S.M. Ahmed, "Investigation of the ring area around cavitation erosion pits on the surface of carbon steel," *Tribol. Lett.* 45, pp. 437–444, 2012.
- [36] W. Wang, X. Zhang, J. Wang, "Pits with colored halos formed on Cr18Ni9Ti stainless steel surface after ennoblement in seawater," *Mater. Sci. Eng. C* 29, pp. 851–855, 2009.
- [37] M. C. Pereira, J. W. J. Silva., H. A., Acciari, E. N., Codaro L. R. O., Hein, "Morphology characterization and kinetics evaluation of pitting corrosion of commercially pure aluminum by digital image analysis," *Mat. Sci. and Applic.* 3, pp. 287-293, 2012.
- [38] J.H. Espina-Hernandez, F. Caleyó, V. Venegas, J.M., Hallen, "Pitting corrosion in low carbon steel influenced by remnant magnetization," *Corrosion Science* 53, pp. 3100-3107, 2011.
- [39] K., Xiao, C.F., Dong, X.G., Li, F.M., Wang, "Corrosion products and formation mechanism during initial stage of atmospheric corrosion of carbon steel," *J. Iron Steel Res. Int.* 15(5), pp. 42-48. 2008.
- [40] N. D. Budiansky, J.L. Hudson, J.R. Scully, "Origins of persistent interactions among localized corrosion sites, Symp. in Honor of Hans Bohni," *Electrochemical Society*, Salt Lake City, UT, 20023.
- [41] D. A., Moreno, J. R., Ibars, C. Ranninger, "Influence of microstructure on the microbial corrosion behaviour of stainless steels", *Rev. Metal. Madrid.* 36, pp. 266-278, 2000.
- [42] *Rust Bulletin* July 15, 2010 <http://www.rustbullet.com.au/technical/how-it-works/introduction-to-corrosion-and-process>.
- [43] X. Kui, D. Chao-fang, L., Xiao-gang, W., Fu-ming, "Corrosion products and formation mechanism during initial stage of atmospheric corrosion of carbon steel," *J. of Iron & Steel Res., Int.* 15(5), pp. 42-48, 2008.
- [44] S.A. Karrab, M.A. Doheim, S. Mohamed, S.M. Ahmed, "Effect of heat treatment and bath composition of electroless nickel-plating on cavitation erosion resistance," *J. Eng. Sci. Assiut Univ.*, 4, pp. 1989-2011, 2013.
- [45] L.L. Shreir, "Tantalum-platinum and titanium-platinum bi-electrodes anodic behavior in electrolytes of low conductivity," *Platinum Metals Rev.* 4(1), pp. 15-17, 1960.
- [46] B. Vyas, and C.M. Preece, "Stress produced in a solid by cavitation," *J. Appl. Phys.*, 47(2), pp. 5133-5138, 1976.
- [47] B., Saleh, A. Abouel-Kasem, A. Ezz El-Deen, S.M., Ahmed, "Investigation of temperature effects on cavitation erosion behavior based on analysis of erosion particles," *Trans. ASME J. Tribol.* 132, pp. 031601, 2010.
- [48] S. Takasaki, and Y. Yamada, "Effects of temperature and aggressive anion on corrosion of carbon steel in potable water," *Corrosion Science*, 49, 240-247, 2007
- [49] J. R. Davis, K. M. Mills, S. R. Lampman, "Metals handbook. 10th edition Vol. 1. Properties and selection: Irons, steels, and high-performance alloys. ASM International, Materials Park, ISBN: 0-87170-378-5 and 0-87170-377-7, 1063, 1990.
- [50] Z. Szklarska-Smialowska, "Pitting Corrosion of Metals", NACE, Houston. 1986.
- [51] G. Wranglen, "Pitting and sulphide inclusions in steel," *Corrosion Science*, 14, pp. 331–349, 1974.
- [52] D. Noah, N.D. Budiansky, J.R. Scully, 2004 "Origins of persistent interaction among localized corrosion sites on stainless steel. *J. Electrochem. Soc.* 151(4), pp. 233-243, 2004.
- [53] G. S. Frankel, "Pitting corrosion of metals, a review of the critical factors," *J. Electrochem. Soc.*, 145 (6), pp. 2186-2198, 1998.
- [54] S.A. Karrab, M.A. Doheim, S. Mohamed, S.M. Ahmed, "Study of cavitation erosion pits on 1045 carbon steel surface in corrosive waters," *trans. ASME, J. Tribol.*, 134, pp. 011602, 2012.
- [55] Z. Tong-He, W. Yu-Guang, L. Xu. An-Dong, W.M, Xiao-Yan, "Nanostructure and properties of corrosion resistance in C+Ti multi-ion-implanted steel," *Chinese Phys. Lett.* 20, pp. 1548-1551, 2003.
- [56] Y. Jang, B. Collins, J. Sankar, Y., Yun, "Effect of biologically relevant ions on the corrosion products formed on alloy AZ31B: An improved understanding of magnesium corrosion," *Acta Biomaterialia* 9, pp. 8761-8770, 2013.